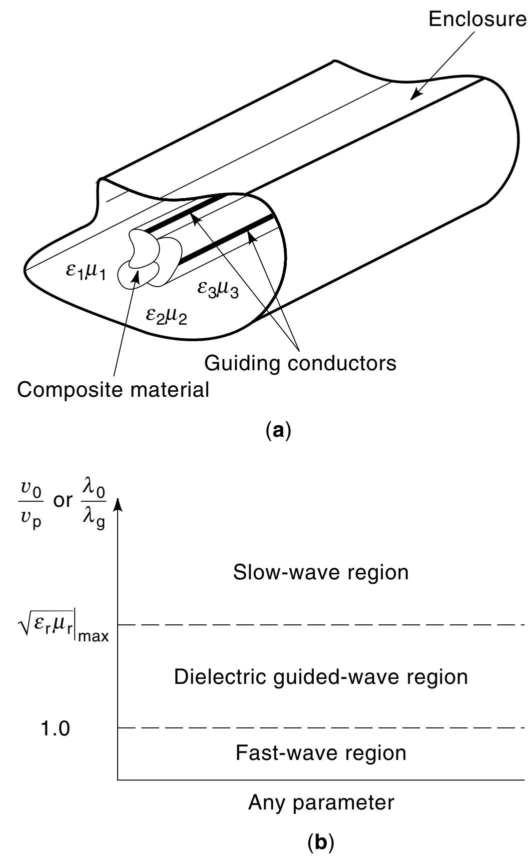

Figure 1. Graphic illustration of a generalized waveguide problem and its guided waves. (a) Physical view of an arbitrary waveguiding structure and (b) concise description of any potential guided-wave propagation along its axial direction, which are classified in terms of three types of waves: slow wave, dielectric guided wave and fast wave. The waveguide consists of a composite medium with three blocks of different relative permittivities ϵ_r and permeabilities μ_r with the subscript r denoting 1, 2, and 3. The outer enclosure may be in the form of a dielectric or metallic boundary. The classification of guided waves is made by measuring the free-space counterpart v_0 relative to its guided wave phase velocity v_p, or equivalently the free-space wavelength λ_0 versus the guided-wave wavelength λ_g. The abscissa in (b) refers to any susceptible physical and electrical parameter connected with wave propagation.

SLOW WAVE STRUCTURES

GUIDED WAVES AND WAVEGUIDES

Electromagnetic wave propagation, which is fundamentally governed by Maxwell's field equations, is usually characterized by its propagation constant. The propagation constant is used to derive its phase and group velocity and attenuation relative to frequency or wavelength. The phase velocity of a freely propagating wave is reduced or increased compared with the speed of light if such a propagation takes place in material other than air or vacuum. Guided-wave phenomena (1–4) are electrically or magnetically bounded waves propagating in air- or material-filled tubes or strips, or called waveguides or sometimes transmission lines, and are the physical foundation for designing and manufacturing radio-frequency (RF), microwave, and optical components and systems. A waveguide can also be defined as a structure that causes a wave to propagate in a chosen direction because of some measure of confinement in the plane transverse to the direction of propagation. The topological view of a waveguide is graphically sketched in Fig. 1(a), which may involve materials of different properties and multiple conductors with or without a specifically shaped dielectric or conducting enclosure. Dielectric guides, hollow-pipe waveguides, and planar guides are the most important building blocks in practical use to date.

Generally, the guided-wave properties of a waveguide depend on physical aspects, such as boundary conditions, materials, and frequency. Conventional uniform waveguides (rectangular metallic waveguides without physical variations in the longitudinal direction, for example) exhibit phase velocities of wave propagation greater than the velocity of light, or in other words, guided wavelengths are longer than the free-space wavelength: these structures are usually called fast-wave structures. Fast-wave structures, in most cases have cutoff frequencies below which wave propagation is halted.

The slow-wave is a particular type of wave propagation, usually of the guided-wave type, and it is described mostly in the frequency domain. Slow-wave structures (5–7) are waveguides or transmission lines in which the wave travels with a phase velocity equal to or less than a certain predesignated velocity of wave propagation. In other words, the slow wave should be interpreted relative to its fast-wave counterpart compared with a velocity of reference, such as the speed of light in a hollow metallic waveguide. However, it may be disputable how to choose the velocity of reference that is directly connected with the slow-wave structure. Of course, one may always choose the speed of light as the reference velocity (classical consideration) to distinguish slow-wave propagation from other guided waves. This was the common practice in very early studies of slow-wave structures probably because the early slow-wave development was closely related to the rectangular and circular waveguiding structures. Since the emergence of planar integrated dielectric-layered geometry, such a classical definition of slow-wave structure was somewhat altered by the relative dielectric and magnetic properties of the materials of the structure. It is now widely accepted that a slow-wave structure can support wave propagation that has a phase velocity less than the attainable value because of the inherent properties of the waveguiding material, such as permittivity and permeability.

Figure 1(b) depicts schematically a concise classification of guided-wave structures by comparing the normalized guided wavelength to its free-space counterpart. We consider the basic waveguiding geometry of Fig. 1(a) as the reference in which the maximum permittivity and permeability of a relevant subregion sets up the border between material-related guided-wave and slow-wave propagation. In most cases, only linear isotropic dielectric materials are used in waveguides. In this description, the slow- and fast-wave guiding properties are simply characterized by a popular technical term called the effective permittivity, which may involve the effect of permeability if the relative permeability is not equal to one, even though the concept of a separate effective permeability is valid.

FUNDAMENTALS OF SLOW-WAVE STRUCTURES

Generally, a slow wave cannot be obtained without artificial guided-wave structures. Special mechanisms in a guided-wave structure need to be designed to generate slow-wave propagation. The basic and absolute condition of a guided-wave structure that supports slow-wave propagation is that this structure should provide separate storage of electric and magnetic energy in space either in the axial or transverse directions. Obviously, any susceptible slow-wave generation depends on the geometry and/or the core materials of a guided-wave structure subject to some particular criteria of construction, that lead to a critical separation of energy in space. The effective spatial separation of electric (capacitive effect) and magnetic (inductive effect) energy constitutes the fundamental principle for designing a slow-wave structure.

There are two fundamental classes of slow-wave structures, several typical examples of which are shown in Figs. 2 and 3. One is the periodic structure (Fig. 2) in the axial or longitudinal direction, and the other consists of uniform structures that have special geometry designed in the transverse direction (Fig. 3). Periodic structures can be formed with two configurations: (a) structures with continuous but periodically varying material properties and (b) structures with periodically loaded sections or periodic boundary conditions. The most common type is the latter. Uniform slow-wave structures usually consist of multilayered or composite materials that have a specially arranged thickness ratio and

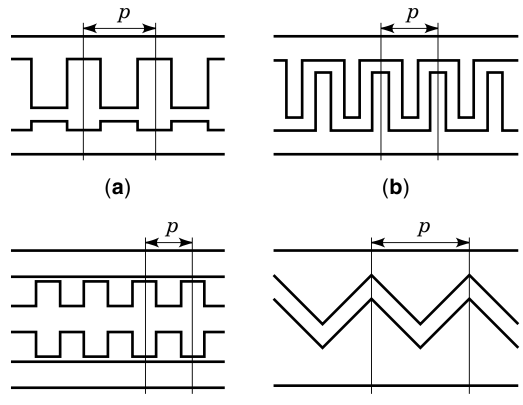

Figure 2. Bidimensional view of generalized periodic slow-wave structures that may depict conventional metallic waveguides and planar transmission lines with a class of typical periodically nonuniform physical layout or patterns (slots or strips) along the propagative axis. p refers to the length of a periodic cell or block. (a) A corrugated waveguide or comb-like line. (b) Either an interdigital line (strip case) or a meader line (slot case). (c) Either a stub-loaded planar line or waveguide. (d) A zigzag nonuniform coupled transmission line.

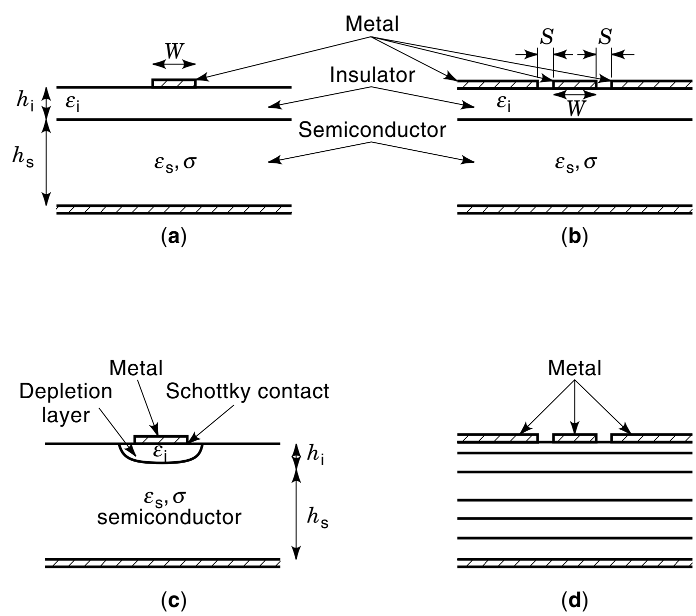

Figure 3. Cross-sectional view of various metal-insulator-semiconductor (MIS) planar slow-wave transmission lines with low-loss or ideally lossless insulator and doped lossy semiconductor. (a) An MIS microstrip structure. (b) An MIS coplanar waveguide (CPW). (c) A Schottky-contact slow-wave microstrip line with a depletion layer that can be regarded as a special case of the MIS structures. (d) A general multilayered planar structure that may involve quantum-well layers. This structure is subject to slow-wave propagation. Mathematical symbols used in the figure are as follows: w and s stand for the widths of the center conductor and slot, respectively. Subscripts i and s refer to the insulating and semiconductor layers, respectively. ϵ is the dielectric permittivity, σ is the conductivity of the doped semiconductor, and h is the thickness of layer.

dielectric/magnetic property. The best known example today in this category is probably the metal-insulator-semiconductor (MIS) transmission line described by the examples of Fig. 3. In this case, planar transmission lines are deposited onto a very thin insulator that is formed, depleted or grown, by using a semiconductor microfabrication process on an appropriately doped semiconductor substrate. Interestingly, slow-wave generation in periodic structures is achieved by separating electric and magnetic energy in the longitudinal space whereas the uniform structures, such as MIS lines, use storage of electric and magnetic energy separated in the transverse direction.

Based on the building block, periodic structures usually require a three-dimensional (3-D) description, whereas uniform slow-wave structures are simply two-dimensional (2-D) problems. The slow-wave characteristics of the two classes of structures differ in some aspects, but they also share some common features. Slow-wave propagation is related to particular electromagnetic modes of the structure, and its fundamental characteristic parameters are the slow-wave factor and propagation loss even though they may be represented differently in some cases. As for other conventional waveguides or transmission lines, characteristic impedance is useful for design purposes but it may be difficult to define for some structures. To accurately describe the guided-wave properties of slow-wave structures, Maxwell's field equations are required to calculate the electrical parameters and to plot the distribution of the field quantities over the structures. The calculation is usually done numerically except for some classical periodic waveguides. These are typical boundary value problems. Normally, the guided-wave properties of a slow-wave structure are dispersive or frequency-dependent, and they can also be greatly modified by changing structure parameters, which are of paramount importance for design purposes.

Now, let us consider some physical aspects of slow-wave structures via two classical examples of periodic structure (see Fig. 4), helix and cavity-chain waveguide, and two popular examples of MIS structures (see Fig. 3), the coplanar waveguide (CPW) and the Schottky-contact microstrip line. Of course, slow-wave generation along MIS structures differs but its physical principle remains similar to that of periodic structures.

A practical helical slow-wave structure typically consists of a metal wire or tape wound in the form of a helix, supported by a longitudinal dielectric rod/bar. The entire structure may also be enclosed in a dielectric/metallic envelope, depending on its intended use. Figure 4(a) shows a typical geometry for a single-tape or single-wire helix that was studied by J. R. Pierce (10) and S. Sensiper (11). The field is guided at the velocity of light along the helical path if no dielectric rod is involved, so that the velocity along the axial or z-direction is considerably less than the velocity of light. Obviously, the tighter the helix is wound, the smaller the pitch p, and the more slowly the wave appears to travel in the axial direction. If an electron beam introduced into the above structures travels along the axis with the same axial velocity as the wave, cumulative field interactions take place, and we have a form of traveling-wave tube. Interestingly, the induced inductance over one helical period prevails over the capacitance, leading to the separation of electric and magnetic energy in the axial direction.

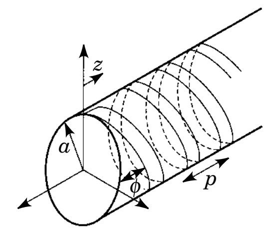

(a)

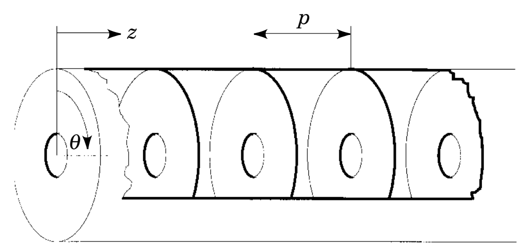

(b)

Figure 4. Two examples of classical periodic waveguides. (a) A simple helix slow-wave structure made of tape or wire. p is the pitch, θ the pitch angle, and a the radius. (b) A periodically disk-loaded (cavity-chain) circular waveguide. p is the periodic spacing of the disks. In both cases, z is the propagation direction of the slow waves.

Figure 4(b) presents an example of metallic waveguides loaded periodically by a series of obstacles, fins in this instance, which slow the wave, as they would slow a stream of water running through the pipe. The smaller the center holes, the greater the reduction in field velocity through the pipe. This structure belongs to the class of cavity-chain, slow-wave structures, each of which consists of a chain of coupled resonant cavities. These cavities are very frequency-selective. Electrons, of course, can be introduced to flow along the axis with a velocity that allows them either to absorb power from or to deliver power to the circuit wave. This mechanism can be used to realize forward-wave traveling-wave amplifiers or backward-wave oscillators, "Carcinatron." Similarly, it can be observed from guided-mode concepts that the spatial separation of electric and magnetic fields satisfy the critical condition of slow-wave guidance.

The basic slow-wave MIS structures consist of planar transmission lines usually in the form of a few or a hundred micrometer-size microstrip, CPW, or other planar patterns, which are fabricated on a doped thin or thick semiconductor substrate, such as N^+ silicon (Si) or GaAs. In an MIS CPW, as shown in Fig. 3(b), the metals are separated from the doped semiconductor by a low-loss or ideally lossless insulating layer, such as silicon dioxide (SiO_2) or silicon nitride (Si_3N_4), that is usually extremely thin and ranges from the submicrometer range to two micrometers. The presence of back metallization usually has a negligible influence on slow-wave propagation, whereas in the Schottky-contact microstrip described in Fig. 3(c), a low-loss depletion region is formed by applying a negative bias voltage over the microstrip with respect to the ground plane. Such a depletion region is equivalent to the insulator of an MIS structure but inhomogeneous in profile over the cross section. Therefore, the Schottky-contact line can be regarded as a special MIS structure. The existence of slow-wave propagation along these MIS structures can be explained in the following manner. The low-impedance doped semiconductor, which is a nonmagnetic material, is virtually invisible to the magnetic field. Therefore, the magnetic field freely penetrates into the semiconductor layer, and it is nearly identical to that of an undoped CPW structure. However, the electric field is highly confined in the insulating layer between the semiconductor and the center strip of the CPW. This field distribution corresponds to separate storage of electric and magnetic energy in space, which is the well-known condition for a slow-wave mode to propagate. Obviously, transmission loss is inevitable and is often the main design problem because MIS structures always contain a doped semiconductor layer. Heuristically, applying different bias voltages on these MIS structures should modify the physical profile of the insulating layer or depletion region, thereby changing the slow-wave propagation. This feature is exploited in designing electronically tunable MIS devices.

A BRIEF HISTORY OF SLOW-WAVE DEVELOPMENT

Based on their classification, the development of the electromagnetic slow-wave structures passed two historical landmarks: the periodic structure and the metal-insulator-semiconductor (MIS) structure. Of course, the MIS structure is not unique for generating slow-wave propagation on the basis of a uniform line made of special material. Slow-wave effects are also observed in waveguides that involve ferromagnetic, plasma, or other complex media, such as chiral materials, if the mechanism and conditions of generating slow-wave propagation in those structures exist. In other words, the spatial separation of electric and magnetic energy takes place.

The very early development of slow-wave structures can be traced back to World War II, when there was an explosion of activity in the microwave electronics field. In 1939, a high-frequency tube, known as the klystron, was developed by W. W. Hansen and the Varian brothers following the invention of the high-power magnetron by A. W. Hull in 1921. At that time, slow-wave structures were built by cascading resonant cavities, which usually provided tremendous power gains over relatively short waveguiding length, but the frequency bandwidth was very limited. These cavity-connected and ladder-type slow-wave structures are still widely used today for highly frequency-selective devices, such as narrowband filters, multiplexers, and field polarization control devices.

In the early 1940s, R. Kompfner (8), reflecting upon the relative inefficiency and narrow bandwidth offered by the klystron, reasoned that if an electron beam were to interact continuously with a wave on a helix, it would interact more efficiently. This is the velocity-matching principle for the electron beam and electromagnetic wave, which are supposed to travel at equal speeds in the ideal case, such that maximum field interaction or energy exchange occurs between the two waves. Furthermore, the helix would not be strongly resonant at any frequency, and therefore it would have a broad bandwidth. Kompfner's first traveling-wave tube (TWT) was successfully developed in 1943, which marked the beginning of slow-wave structures. In fact, a similar concept was proposed but not explicitly described in the patent filed by Percival in 1935 (9) for distributed circuits. Subsequently, the TWT was refined by Bell laboratory workers during and after World War II. Among them, J. R. Pierce is perhaps most prominent. He worked on the TWT theory and built high-performance tubes (10). Since then, a large class of broadband and high-performance traveling-wave electronic devices has been proposed and developed on the basis of various slow-wave structures (11,12). These include distributed TWT amplifiers, oscillators, and linear particle accelerators (13–16). In addition, the slow-wave phenomena were also observed and studied for other classes of structures including plasma- and ferrite-filled waveguides (17). In those early times, periodic structures were sometimes called delay structures instead of slow-wave structures.

Since the mid 1950s, there has been tremendous research and development into planar transmission lines and high-frequency integrated circuits printed on low loss dielectric substrates or semiconductor wafers. These transmission lines may be in the form of microstrip lines, coplanar waveguides (CPW), slot lines, and other derivatives. The concept of hybrid microwave integrated circuits (HMIC)s and monolithic MICs (MMIC)s was eventually proposed in the early 1960s. Such microwave integrated circuits (MIC)s may be designed on lossy semiconductor substrates. Slow-wave propagation along these layered structures was predicted in 1967 (18), and immediately an extensive and detailed study on MIS ($Si\text{-}SiO_2$) slow-wave microstrip lines was published in (19). Subsequently, a Schottky contact microstrip line (20,21) was used as a variable slow-wave structure with an external voltage control.

Periodic structures using planar fabrication techniques had basically received no attention until the emerging design requirement of the broadband or high-directivity microstrip line coupler in the early 1970s. A coupled parallel-line system had been used to design couplers whose electrical performance is usually limited by the mismatch in the phase velocity of the even and odd modes. An effective solution to this problem was introduced by Podell (22), by wiggling the edges of coupled lines. It is used to deliberately control the ratio of capacitance and inductance, leading to the equalization of even and odd mode velocities. This marked the beginning of planar periodic structures that effectively generate slow-wave propagation (23).

Since the early 1970s, research on both MIS and planar periodic slow-wave structures have continued, and a selected set of publications issued before 1987 was presented for MIS-related topics (7). Other published works related to MIS-based and planar periodic slow-wave structures can easily be found in the *IEEE MTT Transactions,* letters and conference publications (*Microwave Theory and Techniques*), *IEE Proceedings* (Part-H), and *Electronics Letters.* Recent advances include (1) the use of hybrid MIS and periodic structures (cross-tie overlay) for low-loss, slow-wave enhancement; (2) the observation of slow-wave effects due to lossy conductor strips at low frequency; (3) the proposal of inhomogeneous doping techniques for improving MIS transmission loss; (4) the development of slow-wave structures using new materials, such as chiral media, photonic band-gap structures, and quantum-barrier traveling-wave devices. Some of these new developments are discussed in a subsequent section. Readers are encouraged to consult those periodicals and publications for more detailed information on this subject.

BASIC THEORY OF SLOW-WAVE STRUCTURE

It is known that periodic and MIS structures yield slow-wave propagation, depending on whether or not the fundamental condition of spatial separation of electric and magnetic energy is sustained. This is to say that slow-wave propagation does not necessarily occur along these structures under certain circumstances. This critical requirement for slow-wave propagation depends in turn on the physical layout of the structure and the working range of frequency. The question is, How shall we describe them electromagnetically at a given frequency and also on which theoretical platform should we rely to predict slow-wave propagation? Furthermore, characteristic parameters must be identified to formulate such guided-wave properties clearly because they are very important for understanding and designing slow-wave structures and circuits.

To begin with, let us consider Figs. 2, 3, and 4, which show a class of planar and nonplanar periodic and MIS structures. We realize first of all that the electric $\vec{E}$ and magnetic $\vec{H}$ fields along these structures should always satisfy Maxwell's equations, which are usually formulated in the frequency domain (angular frequency $\omega = 2\pi f$ and f frequency) for slow-wave guiding structures. Maxwell's field equations are easily found elsewhere (1–4,6). To study guided-wave properties, slow-wave structures are usually assumed to be infinitely long. This stipulation is not just a practical one imposed to simplify matters, as indeed it does, but it turns out that fields and guided-wave characteristics are rather useful and accurate for practical design of a finitely but sufficiently long structure. In addition, results obtained for an infinitely long structure may approach results for its finitely long counterpart quite accurately if both ends are terminated or matched, so as to satisfy the boundary conditions. In this case, the slow-wave structures can be characterized simply by the classical transmission-line theory in a unified lumped-circuit way, that is, the complex propagation constant $\gamma = \alpha + j\beta$ and characteristic impedance Z_0 derived from a generic ladder network are described by its constituent circuit elements *RGLC* that stand for distributed resistance, conductance, inductance, and capacitance per unit of length for a uniform line or per period for periodic structures. Guided-wave properties such as γ and Z_0 can be rigorously modeled by applying Maxwell's equations with appropriate boundary conditions. This may call for numerical approaches if simple analytical or closed-form techniques fail to extract the characteristic parameters. This is true in particular for planar periodic and MIS slow-wave structures.

A unified transmission line model is introduced for both periodic and MIS structures because they can be considered special classes of transmission lines. In addition, it can be shown that transmission line theory (circuit aspect) is consistent with Maxwell's equations (field aspect) for such guided-wave structures. This model mathematically confirms the origin and existence of slow-wave propagation once an effective spatial separation of electric and magnetic energy takes place. In addition, it should reveal some guided-wave properties of the slow-wave structure. Based on the difference in geometry compared with the uniform MIS slow-wave line, the periodic structure may be subject to some unique mathematical theorems and treatments, which are described following, together with other pertinent definitions frequently used with slow-wave structures.

Periodicity or Floquet's Theorem

The periodicity theorem helps us to formulate the guided-wave properties of a linear, periodic, slow-wave system, that is, to determine modes of electric and magnetic fields subject to periodic boundary conditions. This theorem is sometimes called Floquet's theorem, a generalized mathematical theorem for differential equations with periodic coefficients. A *mode* denotes a particular solution to Maxwell's equations or to the wave equations at a certain frequency. A slow-wave could be composed of a number of modes in a hybrid form called hybrid mode, depending on the nature of the structure. The electric and magnetic fields over the cross section should be identical for the infinitely long helix and periodic waveguide, but with a phase shift given by the factor $e^{-j\beta p}$ from any point z to the point $z + p$, where β and p are the fundamental propagation constant and the periodic length, respectively. Without loss of generality, let us consider only electric fields in a Cartesian coordinate system for the periodic cavity-chain waveguide. Floquet's theorem in Cartesian coordinates states that

$$\vec{E}(x,y,z+p) = \vec{E}(x,y,z)\cdot e^{-j\beta p} = \vec{E}(x,y,z)\cdot e^{-j\beta_n p}$$
$$\beta_n = \beta + \frac{2n\pi}{p} \tag{1}$$

in which $n = 0, \pm 1, \pm 2, \pm 3, \ldots$ and so forth, which stand for the index terms of space harmonics. This equation suggests that the electromagnetic solution to a periodic cell with space-harmonic expansion constitutes the completeness of a field solution for the entire periodic structure. Equation (1) implies that "local" waves contained to some extent in the periodic cells that interact with "guided" waves eventually yield a space separation of electric and magnetic energy. The exponent says that the nth mode has a propagation constant β_n on the basis of a Fourier (space harmonic) expansion and that the periodic phase shift of the structure is always dictated by the term or βp or φ.

The determination of β at a given frequency ω is the central problem in a periodic slow-wave structure. The solution is sometimes called the ω–β diagram, or dispersion curve. Note that the concept of a space harmonic differs from that of a mode in that a space harmonic is the inseparable component of a wave containing the explicit exponent factor and it may be a component of a mode. A single space harmonic rarely satisfies all of the boundary conditions, and it may or may not satisfy Maxwell's equations. Nevertheless, under some circumstances the space harmonic expansion may correspond directly to the modes. Sometimes in the literature, this expansion of fields over a periodic cell is called spatial harmonics, or sometimes Hartree harmonics, to represent the guided-wave properties of the complete structure.

Of the infinite number of spatial harmonics, half are forward waves, whereas the other half are backward waves. This interesting and useful feature of periodic slow-wave structures is discussed following.

($\omega - \beta$) DISPERSION DIAGRAM AND SLOW-WAVE PARAMETERS

Our general understanding of the behavior of slow-wave structures depends greatly on ω–β dispersion curves, sometimes called the Brillouin diagram. This is a plot of ω against β. In some cases, the phase shift φ ($\varphi = \beta p$) may also be used (ω–φ curves) for periodic structures. This classical graphic

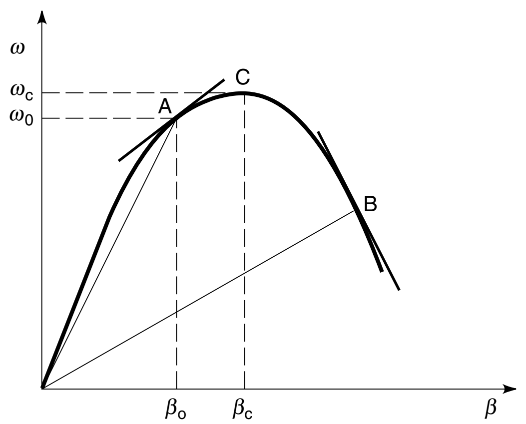

Figure 5. Characteristic dispersion curve, or ω–β diagram, for a slow-wave structure (typically for periodic structures). ω is angular frequency, β propagation constant (usually β is for the fundamental mode of a periodic slow-wave structure). Points A and B represent forward and backward propagating waves in the case of a positive β, respectively, and point C is the cutoff frequency at which energy flow is halted.

representation is popular for periodic structures but not for uniform MIS structures, which use other alternatives, such as a slow-wave factor. Figure 5 depicts a typical ω–β dispersion curve for a slow-wave periodic structure. The phase and group velocities are calculated from

$$v_{\mathrm{p}} = \frac{\omega}{\beta}$$
$$v_{\mathrm{g}} = \frac{\partial\omega}{\partial\beta} \tag{2}$$

The phase velocity v_{p} of a mode is the velocity with which an observer must travel to keep in step with this mode, and it stands for the phase transmission characteristic of each frequency relative to the frequency of reference. Usually, v_{p} differs from mode to mode on the basis of Floquet's theorem. The group velocity v_{g} yields the energy transmission (or power flow) velocity at a finite frequency. The concept of dispersion is used to measure the degree of field variation over the cross section or periodic cell of a structure as the frequency changes. If v_{g} remains constant over a range of frequency, signal information carried by these frequencies travel with the same velocity in the structure. In other words, a structure may be dispersionless if its ω–β curves are simply straight lines or the two characteristic parameters are linearly related to each other. Interestingly, in a periodic structure, the group velocity is the same for all the modes because $\partial\omega/\partial\beta_{\mathrm{n}} = \partial\omega/\partial\beta$ is always satisfied according to Eq. (1). Thus the group velocity is a parameter for an entire wave. If β is positive in Fig. 5, v_{g} is positive at point A, meaning that the signal power flows in the $+z$-direction (forward wave) whereas v_{g} negative at point B means that the signal power flows in the $-z$-direction (backward wave). At point C, the wave is cut off or in a state of local resonance where v_{g} becomes zero. The forward and backward waves are the fundamental physical attributes of periodic waveguides. Obviously, the forward and backward waves are not related only to positive β.

Figure 6 gives a set of ω–φ dispersion curves for a typical periodic waveguide structure. The fundamental forward and backward slow waves are described in Fig. 6(a) and Fig. 6(b), respectively, via the sign of β and slope of ω–φ dispersion curves relative to the space harmonics. There are two possible

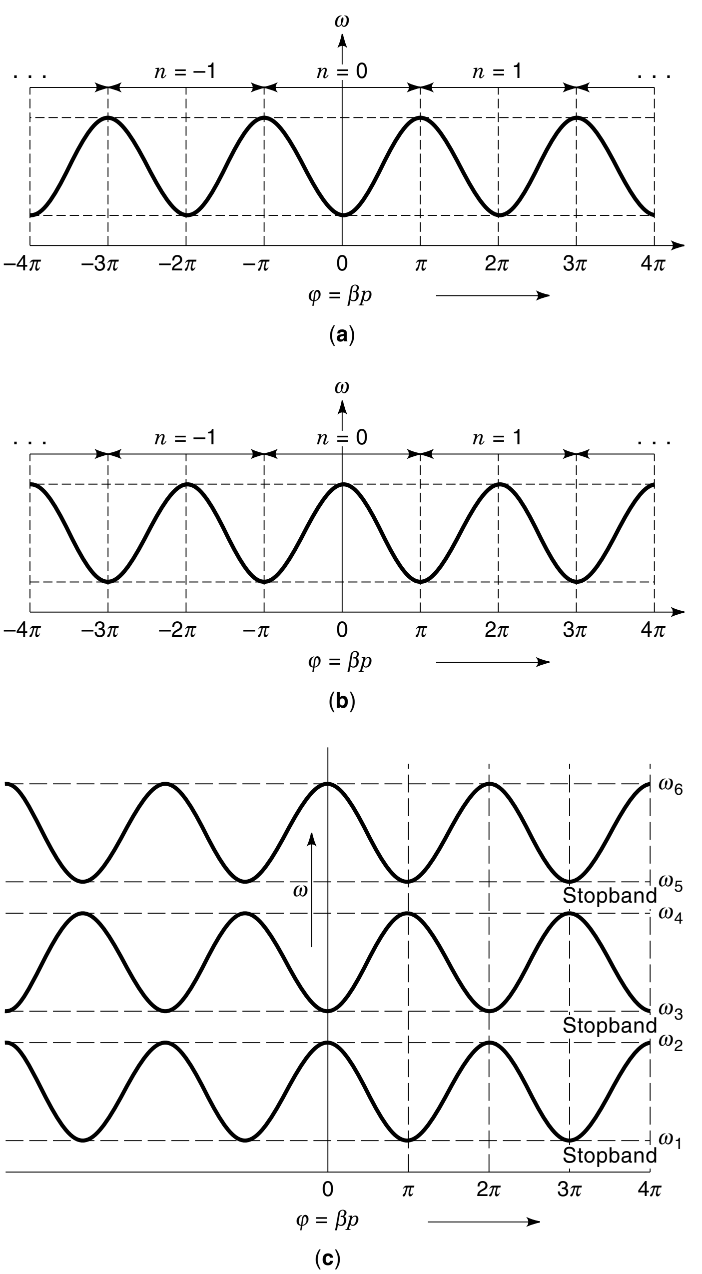

Figure 6. A general form of ω–φ dispersion curve, or Brillouin diagram, for a typical periodic waveguide structure. (a) Forward wave ω–φ relationship and curve slopes for space harmonics with the energy flowing in the $+z$-direction ($\beta_{\mathrm{n}} = \beta + 2n\pi/p$) for the solid lines; and with the energy flowing in the $-z$-direction ($\beta_{\mathrm{n}} = -\beta + 2n\pi/p$) for the dotted line. (b) Backward wave ω–φ relationship and curve slopes for space harmonics with energy flowing in the $+z$-direction ($\beta_{\mathrm{n}} = -\beta + 2n\pi/p$) for the solid lines, and with energy flowing in the $-z$-direction ($\beta_{\mathrm{n}} = \beta + 2n\pi/p$) for the dotted line. (c) Composite $\omega - \varphi$ diagram showing alternated passbands and stopbands. The first three characteristic curves feature forward and backward spatial harmonics. The bandwidths of the three stopbands are not necessarily the same.

scenarios for realizing forward waves as shown in Fig. 6(a): (1) the dispersion curves have positive slopes ($v_g > 0$, and the energy propagates in the $+z$-direction) because $\beta_n = \beta + 2\pi n/p$; or (2) the dispersion curves have negative slopes ($v_g < 0$, and the energy propagates in the $-z$-direction) because $\beta_n = -\beta + 2\pi n/p$. Obviously, forward wave propagations take place if and only if $\partial\omega/\partial\beta_n = \partial\omega/\partial\beta$ and ω/β have the same sign at a given frequency. Similarly, there are also two corresponding scenarios for achieving backward waves, as shown in Fig. 6(b): (1) the dispersion curves have positive slopes ($v_g > 0$, and the energy propagates in the $+z$-direction) because $\beta_n = -\beta + 2\pi n/p$; or (2) the dispersion curves have negative slopes ($v_g < 0$, and the energy propagates in the $-z$-direction) because $\beta_n = \beta + 2\pi n/p$. In this case, the backward wave propagations take place if and only if $\partial\omega/\partial\beta_n = \partial\omega/\partial\beta$ and ω/β have opposite signs at a given frequency. It is helpful to remember that the propagative direction of the fundamental mode guidance differs from that of the energy flow. Based on the difference of dispersion curve behavior between the two classes of waves ($\beta = 0$, for example), the slow wave structure design for forward wave propagations may differ from those of backward waves. The forward wave structures have been used to design amplifiers, such as TWT, usually on the basis of the fundamental mode ($n = 0$). The space harmonics ($n \neq 0$) are often involved in spurious field interactions. The backward wave structures have been popular in designing voltage-controlled oscillators. Space harmonics ($n \neq 0$) could sometimes be used to obtain lower control voltages.

Figure 6(c) shows a composite diagram or general form of ($\omega - \varphi$) dispersion curve, which involves the frequency response of spatial harmonics for three characteristic curves. A transverse electric and magnetic (TEM)-mode periodic line may be considered when $\omega_1 = 0$. Otherwise, this is for a non-TEM mode structure. The frequency ranges between the extremes of an ω–φ curve are called passbands, that is ω_1–ω_2, ω_3–ω_4, and ω_5–ω_6 because β_0 is real and the fields carry real power through the structure. A frequency range between two passbands is a stopband, that is 0–ω_1, ω_2–ω_3, and ω_4–ω_5 within which no real power can flow because the fields decay exponentially away from the reference source. This important feature is of considerable significance in designing filters and other components based on periodic structures.

Passband and stopband characteristics are unique for periodic structures. In the MIS structures, the wave propagation depends, first of all, on the fundamental characteristics of a planar line. A microstrip line is different from a slot line (7,27), for example. The slow-wave characteristics of a MIS structure are characterized by a complex propagation constant and a complex characteristic impedance. In turn the complex propagation constant can be expressed by the slow-wave factor η and loss α in dB/mm. The slow-wave factor is simply defined as

$$\eta = \frac{v_0}{v_p} = \frac{\lambda_0}{\lambda_g} = \frac{\beta}{\beta_0} = \sqrt{\epsilon_{\text{eff}}} \tag{3}$$

where λ_0 and λ_g denote the free-space and guided wavelengths, respectively. β_0 and ϵ_{eff} are the free-space propagation constant (or wave number) and the effective dielectric constant, respectively. Obviously, the slow-wave factor, which is identical to the effective index commonly used in optics, can also be applied to the characterization of periodic structures. The central problem in MIS research work is to obtain the highest slow-wave factor possible at higher frequencies, and the lowest line loss is desired. Potential dielectric, ohmic, and radiative losses contribute to the whole loss. Generally speaking, each loss effect is strongly frequency-dependent. In addition, the physical layout may be designed with some expected impedance value. Sometimes, the MIS slow-wave propagation is measured by a quality factor or figure-of-merit as Q as follows:

$$Q = \frac{\eta}{\alpha} \tag{4}$$

There is no consistency in the literature for the definition of Q, which is also defined elsewhere as $(\alpha \cdot \lambda_g)^{-1}$ (32) or $\beta/(2\alpha)$ (25).

Unified Transmission-Line Model

For the periodic and MIS structures shown in Figs. 2, 3 and 4, the slow-wave propagation of a mode can be represented simply by an equivalent transmission-line model with the characteristic lumped elements whether per unit length or per periodic cell, denoted by *RGLC*. Conventionally, R and G (resistance and conductance per unit length) are caused by the longitudinal current flow on the lossy conductor and transverse current dissipation in the dielectric region, respectively. L and C (inductance and capacitance per unit length) are produced by the longitudinal current flow and transverse electric field effect, respectively. Because multiple modes possibly exist in a waveguide, for instance, the periodic waveguides, multiple lossy network topologies are required to characterize different guided-wave properties of these modes, such as low-pass, high-pass, and bandpass prototypes. Nevertheless, any network topology can be theoretically transformed from the fundamental low-pass prototype, shown in Fig. 7. Therefore, a unified transmission-line model can be set up to interrelate lumped line voltages and currents at an interval of a unit or a period, which is very informative in analyzing slow-wave properties.

In the frequency domain, the transmission-line equations (or telegraph equations) can be expressed by

$$\frac{dV(z)}{dz} = -(R + j\omega L)I(z) \tag{5a}$$

and

$$\frac{dI(z)}{dz} = -(G + j\omega C)V(z) \tag{5b}$$

Uncoupling these two equations leads to wave equations for the voltage and current on the line:

$$\frac{d^2V(z)}{dz^2} = \gamma^2 V(z) \tag{6a}$$

and

$$\frac{d^2I(z)}{dz^2} = \gamma^2 I(z) \tag{6b}$$

where $\gamma = \alpha + j\beta = \sqrt{(R + j\omega L)(G + j\omega C)}$ is the complex propagation constant and the complex characteristic impedance of

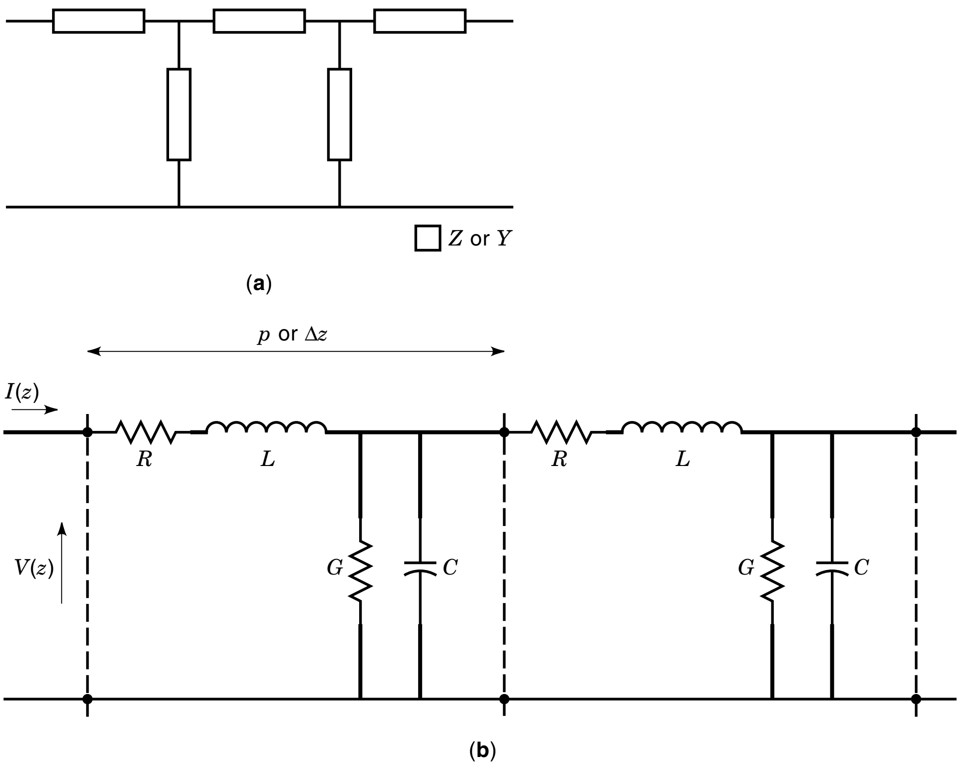

Figure 7. Unified network prototypes or equivalent transmission line model of the slow-wave structures, characterizing frequency responses or guided-wave properties through a set of lumped elements. (a) Arbitrary T or π network representation for any type of slow-wave transmission line. Z and Y stand for complex impedance and immittance, respectively. (b) A general cascaded $RGLC$ lumped-element transmission line model for the periodic and MIS slow-wave structures with the concept of distributed voltages and currents.

the line can be calculated from $Z_0 = Z_{0r} + Z_{0i} = \sqrt{(R + j\omega L)/(G + j\omega C)}$.

The propagation constant may be expanded in a Taylor series to show the asymptotic behavior of the loss and the phase velocity. For high-frequency and low-loss, such that $R \ll \omega L$ and $G \ll \omega C$, the first-order approximation is easily made to obtain the following formulas:

$$\alpha \approx \frac{1}{2}\left(R\sqrt{\frac{C}{L}} + G\sqrt{\frac{L}{C}}\right) \tag{7a}$$

and

$$\beta \approx \omega\sqrt{LC} \tag{7b}$$

Similarly, the complex characteristic impedance can be approximated for low-loss lines such that the real and imaginary parts are given by

$$Z_{0r} \approx \sqrt{\frac{L}{C}} \tag{8a}$$

and

$$Z_{0i} \approx -\frac{1}{2\omega}\sqrt{\frac{L}{C}}\left(\frac{R}{L} - \frac{G}{C}\right) \tag{8b}$$

Of course, the phase velocity of a slow-wave structure can be directly derived from Eq. (7b) via

$$v_p \approx \frac{1}{\sqrt{LC}} \tag{9}$$

This simple equation reveals the fundamental requirements for a guided-wave structure to allow slow-wave propagation: either a large inductance or a large capacitance per unit of length or per period, or both, along the signal path by spatially separating electric and magnetic energy. In a periodic structure, a large reactance (inductance and/or capacitance) is induced by the periodic cell whereas the MIS structure produces only an excess capacitance and its inductance remains basically unchanged with reference to its normal line counterpart. Based on other equations, the loss may be critical in using an MIS structure as opposed to a periodic structure because the lossy semiconductor layer is always required in constructing an MIS structure and both conductance and resistance could be significant at high frequencies. The transmission attenuation of a periodic structure is essentially caused by the conductive (ohmic) loss and potential radiation loss (discontinuity effect). The change in v_p should affect the other line parameters. Consider a helix slow-wave structure that generates a large inductance. Its characteristic impedance may be high, whereas the MIS structure yields a low impedance because of its large capacitance. In fact, the lumped elements can be obtained by approximate and quasi-static models for the slow-wave structures.

APPROXIMATE AND QUASI-STATIC MODELS

Because some slow-wave structures like helical and planar periodic lines are complex, it is rather difficult or even impossible to solve these problems analytically. In the earlier days, high-speed computing resources and modeling capacity were quite limited, and it was not practical to generate tedious field solutions for design purposes. Approximate and quasi-static models that are common in engineering practice were widely used to obtain, within an acceptable margin of error, guided-wave properties and design databases for a large class of slow-wave structures including helical and lumped-element models of planar transmission lines. The approximate models are usually developed on the basis of a much simplified geometry that neglects some physical effects and parameters whereas the quasi-static models are generated simply by considering the limiting case of $f = 0$. The approximate models can be applied to any slow-wave structures, but the quasi-static models are applicable only to those supporting TEM-modes or static field solutions. Generally, all of these models are amenable to simple analytical procedures or sometimes closed-form solutions. Advantages of the quasi-static models are that they allow one to gain insight easily into the slow-wave properties of a structure through its extracted lumped elements.

Because the models and analysis techniques of waveguide slow-wave structures are easily found in the literature and technical books (1,2,6,10,13,14,15,17), our attention in this article is focused on slow-wave models and characteristics of planar structures, which are also recent subjects of interest in research and development. Selected quasi-static and lumped-element models are briefly presented to showcase earlier development of modeling and design tools.

Sheath-Helix Model

Probably, the best known approximate model of periodic structures is the sheath-helix model introduced by P. R. Pierce and then refined by Sensiper. Subsequently, it was extensively used for a large class of helices. This model is not presented in this article because it is well documented in the (6,10,11,14). Other recently published textbooks contain detailed information (2,3). The sheath-helix has dispersion, or $(\omega - \beta)$ curves, that approximate the reality of a helical structure remarkably well. In this model, the actual helix of a finite thickness, whether made of wire or tape, is replaced by a fictitious cylindrical tube model, which has such features as (1) an infinitesimal thickness; (2) a radius equal to the mean radius of the actual helix of finite thickness; and (3) anisotropic conductivity, such that the sheath conductivities are infinite and zero in directions parallel and perpendicular to the helical winding direction, respectively. The sheath-helix model would be closer to the actual situation if the helix is more tightly wound.

Model for Planar Periodic Structure

As a typical and simplified example of planar periodic structures, Fig. 8 shows a linear and isotropic microstrip line consisting of its double-layered geometrical layout with an infinitely thin periodic strip conductor. Its lumped-element equivalence is built on the basis of quasi-static or quasi TEM-mode propagation or low-frequency operation such that the length p of a periodic cell is much smaller than the wavelength. The structure is considered lossless for most quasi-static models even though the ohmic dissipation in a conductor may be significant at higher frequency. Obviously, the wide line section W_1 generates a capacitive effect whereas the narrow line section is responsible for an inductive effect. In this way, the separation of electric and magnetic energy is achieved in longitudinal space, potentially leading to slow-wave propagation. The lumped capacitance C and inductance L per cell section can be effectively calculated and the voltage and current are considered stationary over the periodic section. The phase velocity and characteristic impedance can be readily obtained if L and C are calculated. Therefore, the slow-wave problem is simply reduced to calculations of L and C per periodic cell. The approach, as described in Ref. 23, can be applied to other quasi-static periodic structures.

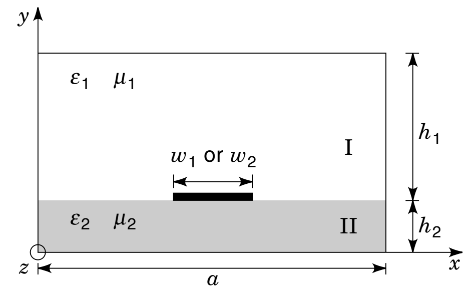

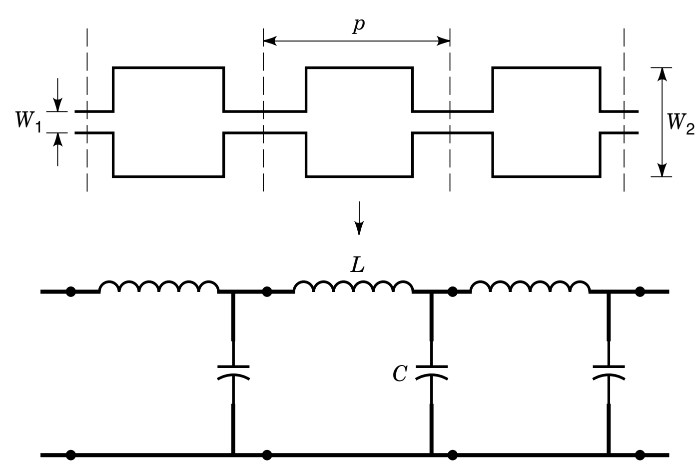

Figure 8. (a) Cross-sectional, (b) longitudinal view and network equivalence of a generalized periodic microstrip slow-wave line sandwiched by two different linear and isotropic dielectric substrates. This periodic line is simply represented by a lumped-element LC model in the absence of both losses and conductor thickness. Geometrical dimensions and substrate parameters sketched in the figure are similar to the previous illustrations. The lumped elements are extracted by an approximate quasi-static model.

Capacitance Calculation. Electrostatic field problems are usually handled via the 3-D Poisson equation which operates on scalar potential functions. With reference to the symmetrical structure of Fig. 8, which is divided into two cross-sectional regions I and II, the periodic cell section is bounded by magnetic walls over which there are no normal electric fields. This is a consequence of the quasi-static condition. The 2-D electric charge density distributed over the periodic conductor surface is denoted by $\rho_e(x, z)$. The electrostatic potentials are expanded in a Fourier series considering boundary conditions. Such expansions are usually in the form of infinite series summations of trigonometric functions, which satisfy the bidimensional boundary conditions over the periodic cells (23).

The infinite summation is subject to a convergence-allowable truncation in numerical calculations. This procedure involves some unknown coefficients. The total energy W_e stored in a periodic section is simply given by $0.5 \int_v \epsilon|\vec{E}|^2\,dv$, in which the electric fields are derived from the scalar potential functions. To eliminate the unknown coefficients, a set of boundary conditions at $y = h_2$ are used. In this case, the coefficients are formulated by $\rho_e(x, z)$. Therefore, the energy is explicitly expressed by

$$W_e = \frac{2}{ap}\sum_{m=1}^{\infty}\sum_{n=0}^{\infty} G_e(m,n) \cdot \left[\int_0^p \int_0^a \rho_e(x,z)\sin\frac{m\pi x}{a}\cos\frac{n\pi z}{p}\,dx\,dz\right]^2 \quad (10a)$$

$$G_e(m,n) = \frac{1}{\delta(n)k_{mn}}(\epsilon_1 \coth k_{mn}h_1 + \epsilon_2 \coth k_{mn}h_2)^{-1} \quad (10b)$$

$$\delta(n) = \begin{cases} 1 & (n \neq 0) \\ 2 & (n = 0) \end{cases} \quad (10c)$$

In Eq. (10b), the term G_e denotes Green's function for this electrostatic field problem. Now, capacitance per periodic section is given by $C = Q/V = Q^2/(2W_e)$ where $Q = \int_0^p \int_0^a \rho^e(x, z)\,dx\,dz$. Q is the total electric charge on the conductor, and it is calculated from the charge density function $\rho_e(x, z)$.

Inductance Calculation. Because of the structural symmetry, the inductance L can be calculated by applying a procedure similar to that for calculating the capacitance. Otherwise, the L calculations are not so simple, and it may require vectorial magnetic potentials that are related to the current density distributed over the conductor. Nevertheless, the magnetic fields in this case have only normal components at the interface $y = h_2$ outside the conductor strip. This is a complementary problem of duality. The scalar magnetostatic potentials proportional to the magnetic fields ($H = -\psi_m$) are used to satisfy the Poisson equation, and they can be expanded with a set of unknown coefficients. At the boundary between the two layers, the normal component of the magnetic flux density is continuous.

In contrast with the electrostatic case, the magnetic flux density is a hypothetical term, and of course, its normal component cannot exist on the conductor surface ($\rho_m = 0$ on the conductor). Similarly, the unknown expanded coefficients can be effectively eliminated, and the total magnetostatic energy is easily obtained by equations in magnetic identity similar to Eq. (10) except that ϵ is replaced by μ^{-1}. The inductance L is given by $L = \Phi/I = \Phi^2/(2W_m)$ with $\Phi = \int_0^p \int_0^a \rho_m(x, z)\,dx\,dz$. Φ is the total magnetic flux interlinking the strip conductor. Because the magnetic flux across one side of the conductor is equal in magnitude and opposite in sign to that over the other side, it can be calculated from the one-side flux density function $\rho_m(x, z)$.

Charge Density Calculation. To complete our calculations of capacitance and inductance, we need to know the electric and magnetic charge density functions. Usually, various techniques connected to the method of moments, such as the Rayleigh–Ritz variational procedure, may be applied to solve this problem. To do so, the unknown charge density functions are expanded in terms of well-behaved basis functions with unknown coefficients, even though the actual charge densities may be very complex. In the C calculation, for example, the electric charge density function may be expressed in terms of known basis functions f_k of finite series such that $\rho_e(x, z) = \sum_{k=1}^{K} \alpha_k f_k(x, z)$, in which α_k are unknown coefficients. The purpose of applying a method of moments is to calculate the unknown coefficients, and then an approximate solution to the problem can be obtained. The L calculation can be made similarly. With the calculated L and C, the slow-wave velocity and characteristic impedance can be derived by applying Eqs. (7–9). The theory and applications of the method of moments can be found in the literature (24). Details on applying the variational principle are described in Ref. 23, which also presents a number of typical theoretical and experimental results of single and coupled microstrip periodic structures.

Model for Planar MIS Structure

Various approximate models were proposed for modeling an MIS microstrip line and CPW, whose cross-sections are shown in Fig. 3 with a unified equivalent circuit model, as described in Fig. 9. Details of these classical techniques are well formulated in technical papers and books, and they include the parallel-plate waveguide model for the microstrip line (21) and the conformal mapping technique for both the microstrip line and the CPW (25). Valid use of these techniques is always subject to careful approximations or assumptions about geometrical dimensions and physical parameters. The Schottky-contact microstrip line, which is regarded as a special case of the MIS microstrip line, can be treated similarly to the MIS structure. Of course, the MIS structure consists of an unavoidable lossy semiconductor layer and an extremely thin insulator usually with very narrow guiding strips. Therefore, the loss is a critical factor in analyzing and designing an MIS structure. There are three potential difficulties encountered in modeling planar MIS structures: (1) accurate characterization of conductor loss; (2) accurate calculation of fringing fields (usually in the case of the parallel-waveguide model); and (3) the quasi-static multilayer model.

Three different modes of propagation exist along an MIS structure as frequency varies (19,21,25), called "slow-wave mode," "dielectric quasi-TEM mode," and "skin-effect mode," respectively. Generally, these modes are roughly distinguished by three characteristic frequencies, namely, the di-

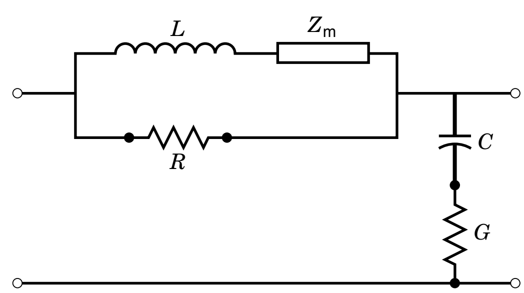

Figure 9. Unified equivalent circuit model for an MIS slow-wave structure including microstrip and CPW lines (see Fig. 3). In addition to the previously defined lumped-elements *RGLC*, Z_m is used to account for the conductor loss, which can be obtained by the calculating surface impedance Z_s, for example.

Table 1. Basic Characteristic Frequencies and Lumped-Element Equations of the Approximate Quasi-Static Model for MIS and Schottky-Contact Microstrip Lines and MIS Coplanar Waveguides (CPW)

Line Type		Lumped Elements						
		f_d	f_s	R	G	L	C	Z_m
Line Type	MIS and Schottky-Contact Microstrip	$\frac{\sigma}{2\pi\varepsilon_0\varepsilon_s}$	$\frac{1}{\pi\sigma\mu_0 h_2^2}$	$\frac{3}{\sigma h_2 w}$	$\sigma\frac{w}{h_2}$	$\mu_0\frac{(h_1+h_2)}{w}$	$\varepsilon_0\varepsilon_i\frac{w}{h_1}$	$\frac{Z_s}{w}$
	MIS CPW	$\frac{\sigma}{2\pi\varepsilon_0\varepsilon_s}$	$\frac{1}{\pi\sigma\mu_0(w/2+s)^2}$	$\frac{1}{\sigma\delta w}$	$2\sigma F$	$\frac{\mu_0}{4F}$	$\frac{\varepsilon_0\varepsilon_i w}{h_1}K$	$\frac{Z_s}{w}$

[a] The model validity may be subject to certain limiting conditions. Physical and electrical parameters refer to Fig. 3. The geometrical factor F is calculated by Eq. (11). The complex impedance of conductor Z_m can be derived from the surface impedance Z_s that can be modeled by several well-documented techniques (see relevant references and literature for more details). The K value, usually slightly greater than 1, is used to assess the effect of fringing fields, and it can be numerically calculated by an exact static model.

electric relaxation frequency f_d, the characteristic skin-effect frequency f_s, and the relaxation frequency of interfacial polarization $f_p = f_d(\epsilon_s h_1)/(\epsilon_i h_2)$ in which the physical parameters are specified in Fig. 3. The lumped-element $RGLC$ depicted in Fig. 9 is easily derived from the quasi-static (TEM-mode) models (19,21,25). Table 1 summarizes quasi-static approximations of the lumped elements for the MIS microstrip (including Schottky-contact line) and CPW. In Table 1, ϵ_0 and μ_0 are the permittivity and permeability of free space, respectively, and F is a geometrical factor stemming from the conformal mapping model, which is approximated by

$$F = \begin{cases} \dfrac{\ln\left[\dfrac{2(1+\sqrt{k})}{(1-\sqrt{k})}\right]}{\pi} & \text{for } 0.707 \le k \le 1 \\ \dfrac{\pi}{\ln\left[\dfrac{2(1+\sqrt{k'})}{(1-\sqrt{k'})}\right]} & \text{for } 0 \le k \le 0.707 \end{cases} \tag{11}$$

in which $k = W/(W + 2S)$ and $k' = \sqrt{1 - k^2}$. The parameter K in Table 1, which can be numerically calculated by an exact static model, accounts for the effect of fringing fields, and its value is slightly greater than 1.0. The effect of conductor loss is reflected in its complex impedance Z_m. It can be derived by several techniques, such as the incremental inductance rule (7), phenomenological loss equivalence (26), and surface impedance approach (7). Other parameters are described in Fig. 3.

ACCURATE AND HYBRID-MODE FIELD MODELS

Accurate field models are usually required when approximate models are no longer valid or the operating frequency is too high to use a quasi-static approximation. In other cases, the use of hybrid-mode field techniques are mandatory because the slow-wave structures cannot support a quasi-TEM mode propagation, such as the corrugated periodic waveguide and the fin line, to name two typical examples. Some physical approximations simplify or make a field model useful before its analytical development. Therefore, the choice of an appropriate field model is critically important for its expected accuracy and efficiency when applied to the structure of interest. There are many techniques available today, whose solutions are usually in numerical form. They include the method of moments, finite-difference and finite-element techniques. Readers are referred to other articles and literature for details on the numerical techniques. There is no "lumped-element" consideration in the field models to account for the spatial separation of electric and magnetic energy in contrast with the quasi-static models.

In the past, a number of efficient techniques were applied to various periodic waveguides (3-D problems) and MIS multilayered planar transmission lines (2-D problems). Earlier models for the waveguide problems were usually related to modal expansion or mode-matching techniques. Planar periodic structures were studied with a spectral-domain approach (27–29), which can also be applied to MIS slow-wave structures. In this case, the conductor thickness is usually assumed to vanish even though its effect may be included in the model. In fact, the conductor loss with a finite thickness in the field-based models can be evaluated by various techniques, such as the surface impedance scheme (7) and the self-consistent technique (30). The semiconductor layer of an MIS structure may be inhomogeneous under certain circumstances, such as a depletion region of the Schottky-contact structures and partially doped MIS lines. Therefore, a generalized technique may be required to handle such complex topologies. In the following, two typical techniques are presented narratively to showcase modeling using field theory.

Model for Planar Periodic Waveguide

Electromagnetic fields in a planar multilayered periodic structure are described by scalar electric and magnetic potential functions that also satisfy Helmholtz equations and boundary conditions (29). Such potentials can be expanded as functions of trigonometric functions in their infinite summations by considering Floquet's spatial harmonic representation in the periodic cell. Similarly to the static model, the infinite summation must be truncated. As detailed in Ref. 29, the Floquet harmonics can be regarded as "modal spectra" in the Fourier sense or as a "natural Fourier transform" in the half-periodic cell ($p/2$). As such, a double Fourier expansion is developed over the planar periodic fin line or slot-line cell along the x–z plane, as shown in Fig. 10. The resulting formulation suggests that a procedure called "higher order resonant harmonic decoupling" can be readily applied, meaning that even- and odd-harmonics in the z-direction ($p/2$) can be separated regardless of the fundamental mode. This argument translates the Floquet's theorem into a linear superposition of the spatial harmonics in a periodic cell with fictitious electric and magnetic walls defined at the periodic boundaries with the interval ($p/2$), as indicated in Fig. 10.

This decoupling procedure provides us with a powerful bidimensional Fourier transform tool in the x–z plane. In addition, this consideration allows predicting the existence of two modes: TM (even harmonics) and TE (odd harmonics). In this way, the Helmholtz equations can be transformed into y-dependent, ordinary differential equations that are solved analytically along the layered transverse direction. This corresponds to a set of transmission-line equations in the spectral domain. The use of the transmission-line equations and additional boundary conditions leads to algebraic, spectral-domain-coupled, Green's function $\tilde{Y}$ in the form of a matrix at the periodic discontinuity:

$$\begin{bmatrix} \tilde{Y}_{xx}(\alpha_m, \xi_n, \beta) & \tilde{Y}_{xz}(\alpha_m, \xi_n, \beta) \\ \tilde{Y}_{zx}(\alpha_m, \xi_n, \beta) & \tilde{Y}_{zz}(\alpha_m, \xi_n, \beta) \end{bmatrix} \cdot \begin{bmatrix} \tilde{E}_x(\alpha_m, \xi_n) \\ \tilde{E}_z(\alpha_m, \xi_n) \end{bmatrix} = \begin{bmatrix} \tilde{J}_x(\alpha_m, \xi_n) \\ \tilde{J}_z(\alpha_m, \xi_n) \end{bmatrix} \tag{12}$$

Obviously, the elements in Green's function are related to α_m (the x-oriented spectral variable), $\xi_n = 2\pi n/p$ (the z-oriented spectral variable), and the unknown β. Then, the unknown aperture fields E and currents J can be expanded in terms of bidimensional basis functions with unknown coefficients, and Galerkin's technique is applied to derive a coefficient matrix equation in the spectral domain.

A nontrivial solution for the propagative constant is obtained by setting the determinant of the coefficient matrix $M(\beta)$ equal to zero. Several algorithms may be applied to search for solutions of this resulting nonlinear equation (eigenvalue problems). As explained in Ref. 29, the basis functions can be defined as functions of two types, namely, "guided" and "stored" basis functions. The field quantities and other parameters can be calculated once the fundamental propagation constant is obtained, leading to the visualization of the field profile over the structure.

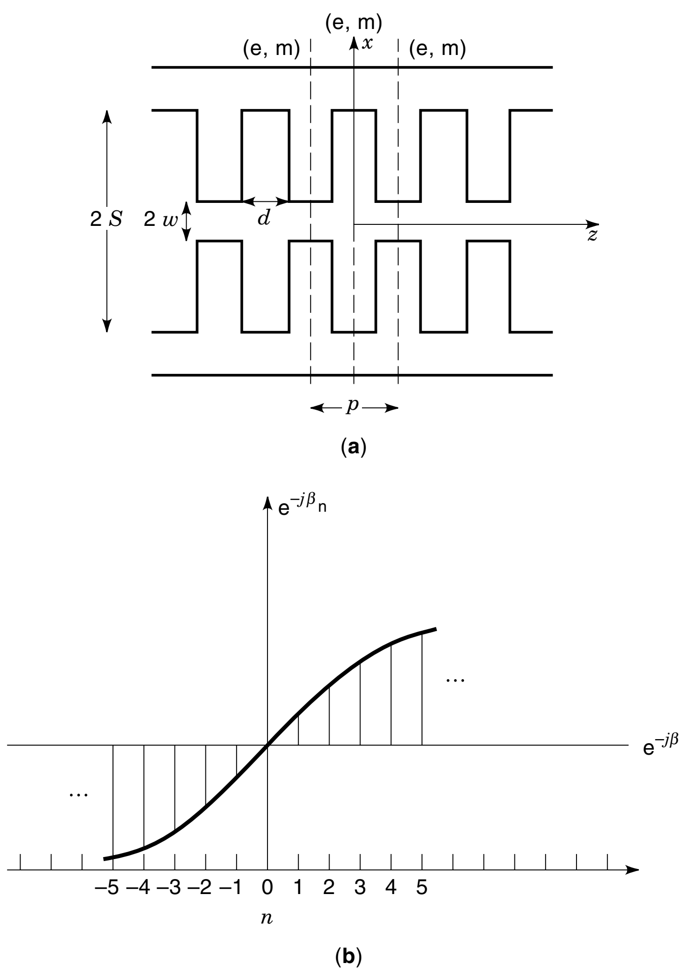

Figure 10. Two-dimensional physical layout description (a) and spatial-harmonics representation (b) of a periodically loaded planar slot line or fin line whose periodic cell is defined by d (the spacing between two adjacent stubs along the axial direction), $2w$ (the gap between the in-line stubs), and $2s$ (the distance between the two bottom lines). The cross section of this structure may be in the form of multilayer dielectrics, whereas the spatial harmonics are transformed into a linear superposition of even (magnetic) and odd (electric) harmonics in a single periodic cell for a hybrid-mode model.

Model for Planar MIS Structure

Because the MIS structures are a class of typical planar lossy transmission lines with a multilayered dielectric, a broad range of field-based techniques can be applied. However, the spectral-domain approach, the method of lines, and the mode-matching technique are the widely accepted schemes for modeling these structures because the MIS structures have such special features that the ratio of thickness among the multiple layers is relatively large and also the line width may be critically small compared with other structures. In addition, an inhomogeneous doping profile is possible for improving line performance (31). Therefore, those fine details must be efficiently taken into account if a successful model is to be obtained. These arguments recommend that a model free of space discretization from layer to layer is favored, which includes the previous schemes. The following presentation is limited to an overview of the method of lines (32), which is a popular alternative to the spectral-domain approach when applied to the same problem. In particular, this method has some unique features, and it allows handling complex cross-sectional geometries, as in an inhomogeneously doped layer.

To begin with, an ideal lossless guiding conductor of vanishing thickness is considered for simplifying the model description. The same field equations as in the modeling of planar periodic structures are used herewith with the two potential functions. The whole MIS structure depicted in Fig. 3 is sampled by a set of alternate electric and magnetic lines perpendicular to the conducting strip plane. The potentials of each of the sampling lines must satisfy the Sturm–Liouville and Helmholtz equations. The Sturm–Liouville equations allow one to account for an inhomogeneous profile (32). Using finite-difference techniques, these partial differential equations are cast into spatially coupled ordinary differential equations for each layer of the MIS guiding structure. Then they can be decoupled by matrix diagonalization via matrix eigenvalue techniques to yield simple transverse transmission-line equations.

In our model, the lower boundary is a perfect electric wall under the ground plane whereas the upper boundary may be infinity, corresponding to a matched transverse transmission line. Starting from both boundaries with the aid of transverse transmission concepts, we enforce field continuity at each interface. Finally, by equating the upper and lower tangential field components at the entire interface of the conducting strip, a characteristic matrix relationship may be derived from the matrix transformation back in the original space domain. Extracting the sampling lines that intersect the conductor over which the tangential electric fields are null, we obtain a smaller matrix. The complex propagation constant is obtained from its nontrivial solution.

In contrast with the spectral-domain approach, the method of lines is always formulated in the semi-discrete space domain. The underlying advantages are its rigorous approach, simple convergent behavior, and fast algorithm with small memory requirements.

SLOW-WAVE SUMMARY AND APPLICATIONS

The two classes of slow-wave structures discussed previously, periodic structures and MIS transmission lines, have their own distinct characteristics because the mechanism of generating slow-wave propagation differs in separating electric and magnetic energy in space. The difference between them can be largely seen from their parameters, such as the slow-wave factor, transmission loss, characteristic impedance, bandwidth, frequency response, dispersion, and power handling capability. Modeling strategies for both types also differ. In fact, different groups of periodic structures and MIS lines also exist, based on the fundamental building block's geometry. The hybrid periodic MIS structures (sometimes called cross-tie overlay MIS structures) are also interesting in their own right, because they share some of the common characteristics of both periodic and MIS structures.

Slow-wave structures are characterized theoretically and experimentally for design purposes. There are several experimental techniques available, such as classical measurement methods for both periodic and MIS structures (7,29). Other alternative methods, such as the ring-resonator technique, electro-optical sampling, time-domain measurements, and on-wafer probing techniques are also useful. Figure 11 shows an example of the measurement test setups for periodic structures, which allow one to extract the slow-wave factor and transmission loss.

Slow-wave structures are very useful in practice and play roles of paramount importance in the electrical and electronic fields. They are used and will continue to be used in diversified applications, including a broad range of passive and active circuits and devices in radio-frequency, microwave and millimeter-wave, and light wave technologies. Now, slow-wave structures are categorized in terms of guided-wave properties, and various applications are also presented to highlight the importance of slow-wave structures in high-frequency electromagnetic engineering.

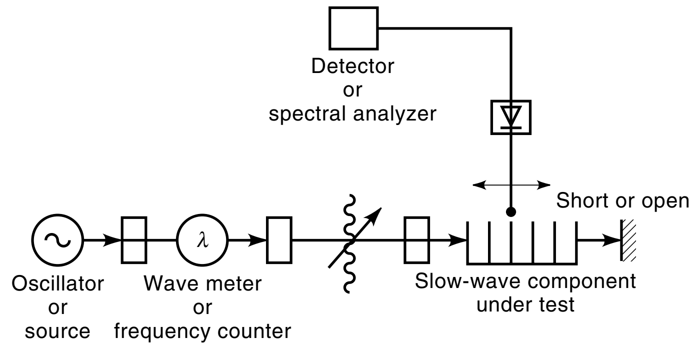

Figure 11. An example of the illustrative measurement setup of a conventional experimental procedure for a periodic structure in the frequency domain.

Slow-Wave Structures and Properties

Periodic Structures. There are two classes of periodic structures: nonplanar and planar. The nonplanar structures include metallic waveguides, coaxial lines, and dielectric waveguides whereas the planar structures are related to the integrated planar dielectric layers on which periodic metallic patterns are formed or printed. The periodic structures have quasi-periodic frequency response in the form of bandpass and band-stop (see Fig. 6 and Ref. 28 for an illustration) and they are quite dispersive. Low-loss, slow-wave transmission usually occurs in the band-pass region, and the structures may exhibit relatively high dispersion. A broad range of characteristic impedance and bandwidths are achievable on the basis of flexible and simultaneous separation of electric and magnetic energy in space. The nonplanar periodic structure may provide high-power handling capability and high-Q (low-loss) over its planar counterpart.

Three categories among the periodic structures in the form of nonplanar structures that have a relatively long history: the helix, the periodically obstacled waveguide, and the serpentine line. Planar structures may have similar periodic patterns, but they are formed on the 2-D plane whereas the nonplanar structures have 3-D features, and they are more flexible in structural design.

The helix (wire or tape) has continued to enjoy widespread use since its inception in a TWT. Three typical structures of the helix are the simple helix, the bifilar helix, also called the folded helix, made of two contrawound helices of equal but reversed pitches, and a ring-and-bar structure (14). The last two helix-derived structures may have improved performance over the simple helical structure, such as higher allowable voltage, better thermal conditions, higher interactive impedance, and higher gain, when used in a TWT. However, the simple helix has the largest bandwidth. Similar helical patterns could also be realized by planar means but very few examples are known to date because they are not useful for high-power applications.

Periodic waveguides supporting non-TEM modes usually behave as high-pass or band-pass filters, depending on the geometry of periodic obstacles or patterns. The topological form of such periodic obstacles characterizes the slow-wave properties. Typical examples include cavity-to-cavity chain structures. The intercavity couplings are made through capacitive or inductive schemes with various shapes, such as slot, cloverleaf, annular ring, and disk. Using the planar technique, the cavity can be easily made in the form of a patch or other geometry, and it can be coupled via gaps and other means.

Some typical examples of the serpentine line structure are the folded waveguide, including the meander-type line and the interdigital structure. Obviously, these structures can be realized easily by planar techniques. A number of these lines exhibit TEM-mode slow-wave propagation and usually the dispersion is low over a wide frequency range. Typical stationary field profiles and mode description over the periodic cell are shown in Fig. 12 for a fin-line structure at its fundamental resonance (29).

MIS Transmission Lines. The MIS structures consist of thin- (several micrometers) and thick-film (several hundred micrometers) types on the basis of the thickness of the semiconductor (Si, GaAs or InP) layer. The insulating layer (SiO_2 or Si_3N_4) is always kept very thin at around the order of less than 2 μm. The fundamental characteristics of a MIS structure depend, first of all, on its line pattern. The thin-type MIS line was developed much earlier than its thick-type counterpart. Generally speaking, the thin-type semiconductor layer is less doped than the thick-film for a much higher slow-wave factor, but its dispersion is also relatively high. The thick-type is usually heavily doped and has low dispersion over a wide frequency range. The low-loss propagation of a thick-film type may easily exceed 10 GHz with moderate slow-wave factors and easy-to-match impedance whereas the thin-film type is limited to several GHz. There is also a difference between the normal MIS structures and Schottky-contact lines. Usually, the Schottky-contact line may require a voltage bias for practical use, and it is usually made of a microstrip line even though other lines are still feasible. The normal MIS structures may have any form of line patterns, such as microstrip, CPW, coplanar strip, fin-line and slot-line, and so on.

As mentioned in its lumped-element model, the MIS structure presents three basic characteristic frequencies with which it is convenient to design a "characteristic frequency map" in connection with the doping conductivity and frequency, as shown in Fig. 13. This map indicates the three possible modes of propagation identified in an MIS structure:

1. *Dielectric Quasi-TEM Mode.* This is for the region where $f_d < f < f_s$. In this range, $\omega\epsilon_s > \sigma$ such that the doped semiconductor layer acts like a normal dielectric and confines most of the guided-wave energy in it. The propagation is usually lossy.
2. *Skin-Effect Mode.* When $f_s < f < f_d$, the doped semiconductor layer behaves as a lossy conductor wall to the wave because $\omega\epsilon_s \ll \sigma$. Hence, the depth of penetration or the skin depth $\delta = \sqrt{2/(\omega\mu 0\sigma)}$ becomes smaller than h_2. The propagation is significantly dispersive.
3. *Slow-Wave Mode.* This is for the region where $f \ll f_d$ and $f \ll f_s$ as indicated in the map. In this case, f is perceived as not so "high" with the moderate value of σ. The electric field is confined within the insulator whereas the magnetic field penetrates freely over the cross section, resulting in energy separation in space.

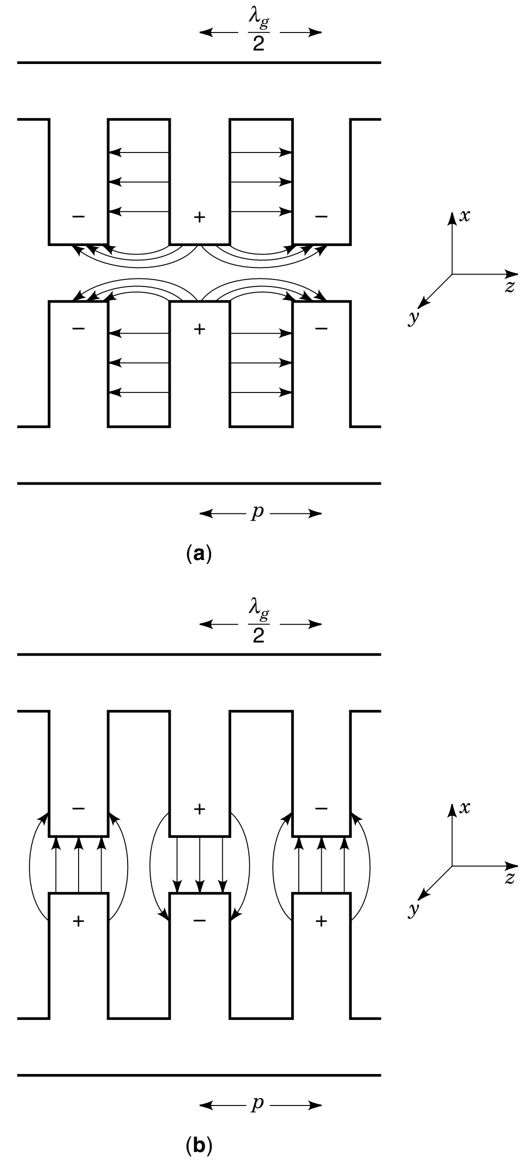

Figure 12. Typical electric field patterns or fundamental mode profiles in the (x–z) section of a resonant periodic slow-wave structure (the periodic length p is equal to half of the guided-wave length $\lambda_g/2$ in this circumstance), which are generated by a hybrid-mode modeling technique. (a) TM_{11} mode; and (b) TE_{10} mode, in the case of a slot-line or fin-line structure, as indicated in Fig. 10.

The conductor loss is an important aspect in designing an MIS structure. The loss may be accurately calculated by a self-consistent approach (30,32). In this case, the conductor of a finite thickness is modeled merely as a normal lossy dielectric layer with intrinsic conductivity. For a MIS line operating in the slow-wave mode, the conductor contributes largely to the total loss at low frequency, over which the semiconductor loss is relatively small.

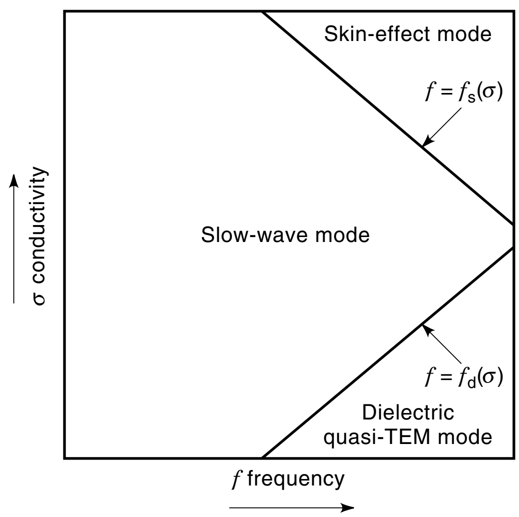

Figure 13. σ–f characteristic frequency map of a typical MIS slow-wave structure (TEM-mode type lines) that characterizes three modes: slow-wave mode, dielectric quasi-TEM mode and skin-effect mode. This symbolic map is useful in designing an MIS structure with preliminary consideration of parametric effects on its slow-wave factor and transmission loss.

Slow-Wave Applications

It is known that slow-waves are not limited to periodic and MIS structures. Other structures that generate slow-wave propagation may be competitive in finding applications. Conductors, including superconductors (30,33), for example, exhibit slow-wave effects at low frequency. In this case, the field may penetrate into the conductor, leading to a significant increase in line inductance. Complex media, such as chiral waveguides, may support slow-wave propagation with specially arranged and coupled electric and magnetic properties to separate electric and magnetic energy. A photonic bandgap structure presents merely periodic lattice geometry, which is also subject to slow-wave propagation. Nevertheless, most slow-wave applications known so far rely essentially on the periodic and MIS structures.

The basic applications for slow-wave structures are usually related to the following uses as passive circuits and active devices: circuit miniaturization, frequency-selective devices and filters, traveling-wave devices, antennas, time-delay lines, phase shift and equalization, impedance match, mode polarization, energy conversion, amplification, oscillation, pulse shaping and signal synchronization. Table 2 presents a general comparison and summary of performance among the periodic waveguides and MIS lines for slow-wave propagation based on the previous discussion. The table provides a critical choice of these structures for various applications, such as high-power traveling-wave devices, integrated microwave circuits, high-speed signal interconnects, optoelectronics, and superconducting devices. Selected devices and circuits are discussed following to highlight some uniquely useful features of slow-wave structures.

Phase Shifter and Delay Line. Both periodic and MIS structures can be used to design these devices as hybrids or monoliths. Usually, the periodic slow-wave structures present fixed-phase shifting and long time-delay lines. In this case, superconducting technology may be used to significantly reduce the intrinsic conductive loss, for example, a physically very long line required to achieve more than several nanoseconds of group delay. Delay-line concepts were developed much earlier with periodic waveguide structures whereas the phase shifter has been a popular research topic using the MIS slow-wave structures, especially in designing tunable phase shifters (34).

Linear and Nonlinear Traveling-Wave Devices. Some classical slow-wave examples are high-power traveling-wave tubes, backward-wave oscillators, amplifiers, and linear accelerators using periodic waveguides. The planar technologies allow designing similar distributed devices based on transistors and nonlinear transmission lines (NLTL) for broadband devices including broadband impedance matching networks, field grating devices, and of course, broadband amplifiers (35). On the other hand, the velocity-match mechanism of electrical and optical signals can be realized by using periodic

Table 2. Critical View and Comparison of High-Frequency Electrical and Mechanical Characteristics of the Periodic and MIS Slow-Wave Structures Judging from Their Passive Circuit Applications

		Basic Characteristics				
		Maximum Limiting Frequency	Transmission Loss	Slow-Wave Factor	Structural Size	Frequency Dispersion
Slow-Wave Structures	Metallic and dielectric periodic waveguides	Extremely high	Very low	Low to moderate	Large to very large	High
	Planar periodic waveguides	High or relatively high	Moderate to low	Low to moderate	Small to medium	Medium to high
	Thin-film MIS lines	Low (several GHz)	Medium to relatively high	Very high	Extremely small (hundred μm)	Relatively high
	Thick-film MIS lines	Medium (possibly up to 30 GHz)	Relatively low	Moderate	Miniaturized to several μm	Low

[a] As compared with the MIS lines, the periodic waveguides present usually bandpass and bandstop characteristics, thereby leading to high dispersion of frequency. On the other hand, the unavoidable lossy semiconductor layer in the MIS structures exhibits adversely higher loss of transmission. The performances of the MIS structures refer basically to the Si–SiO_2 building block. The thin and thick films are distinguished by the thickness of the doped semiconductor, which is in the range of several μm and several hundred μm in thickness of the doped semiconductor, respectively.

electrodes and also the control of MIS slow-wave guidance on traveling-wave electro-optical modulators and photodetectors for wideband applications (36).

Filtering and Pulse-Control Devices. A class of filters and multiplexer can be designed with periodic structures, using their bandpass and band-stop characteristics. Extremely low-loss and linear-phase narrowband filters are realized from superconducting slow-wave lines that have various periodic patterns (37). Frequency-selective devices and some traveling-wave antennas can also benefit from the advantageous features of periodic slow-wave structures. Pulse-control lines, including pulse-shaping devices, are often seen in high-speed digital circuits and interconnects. In this case, the MIS structures may play an important role in designing low-dispersion and signal-synchronized-pulse routine lines (38).

BIBLIOGRAPHY

1. J. C. Slater, *Microwave Electronics,* Princeton, NJ: Van Nostrand, 1950.
2. S. Ramo, J. R. Whinnnery, and T. Van Duzer, *Fields and Waves in Communication Electronics,* New York: Wiley, 1984.
3. R. E. Collin, *Field Theory of Guided Waves,* 2nd ed., New York: IEEE Press, 1991.
4. R. F. Harrington, *Time-Harmonic Electromagnetic Fields,* New York: McGraw-Hill, 1961.
5. L. Brillouin, *Wave Propagation in Periodic Structures,* 2nd ed., New York: Dover, 1953.
6. R. M. Bevensee, *Electromagnetic Slow Wave Systems,* New York: Wiley, 1964.
7. T. Itoh (ed.), *Planar Transmission Line Structures,* New York: IEEE Press, 1987 (see Part X).
8. R. Kompfner, The traveling wave valve, *Wireless World,* **52**: 369–372, 1946; see also The traveling-wave tube as amplifier at microwaves, *Proc. IRE,* **35**: 124–127, 1947.
9. W. S. Percival, *Improvements in and relating to thermionic valve circuits,* British Patent Specification No. 460 562, 1936.
10. J. R. Pierce and L. M. Field, Traveling-wave tubes, *Proc. IRE,* **35**: 108–111, 1947; see also J. R. Pierce, *Traveling Wave Tubes,* 1st ed., Princeton, NJ: D. Van Nostrand, 1950.
11. S. Sensiper, Electromagnetic wave propagation on helical structures, *Proc. IRE,* **43**: 149–161, 1955.
12. A. A. Oliner and W. Rotman, Periodic structures in through waveguide, *IRE Trans. Microwave Theory Tech.,* **MTT-7**: 134, 1959.
13. A. H. W. Beck, *Space-Charge Waves,* New York: Pergamon, 1958. [Vol. 8 of *International Series of Monographs* on Electronics and Instrumentation, D. W. Fry and W. A. Higinbotham (eds.)].
14. B. N. Basu, *Electromagnetic Theory and Applications in Beam-Wave Electronics,* Singapore: World Scientific, 1996.
15. S. Y. Liao, *Microwave Electron-Tube Devices,* Englewood Cliffs, NJ: Prentice-Hall, 1988.
16. A. S. Gilmour, Jr., *Microwave Tubes,* Dedham, MA: Artech House, 1986.
17. A. W. Trivelpiece, *Slow-Wave Propagation in Plasma Waveguides,* San Francisco: San Francisco Press, 1967.
18. H. Guckel, P. A. Brennan, and I. Palocz, A parallel-plate waveguide approach to microminiaturized, planar transmission lines for integrated circuits, *IEEE Trans. Microwave Theory Tech.,* **MTT-15**: 468–476, 1967.
19. H. Hasegawa, M. Furukawa, and H. Yanai, Properties of microstrip line on Si-SiO_2 system, *IEEE Trans. Microw. Theory Tech.,* **MTT-19**: 869–881, 1971.
20. J. Jaffe, A high-frequency variable delay line, *IEEE Trans. Electron Devices,* **ED-19**: 1292–1294, 1972.
21. D. Jäger, Slow-wave propagation along variable Schottky-contact microstrip line, *IEEE Trans. Microw. Theory Tech.,* **MTT-24**: 566–573, 1976.
22. A. Podell, A high directivity microstrip coupler technique, *1970 G-MTT Symp. Digest,* 1970, pp. 33–36.
23. T. Sugiura, Analysis of distributed-lumped strip transmission lines, *IEEE Trans. Microw. Theory Tech.,* **MTT-25**: 656–661, 1977.
24. R. F. Harrington, *Field Computation by Moment Methods,* Malabar, FL: Krieger, 1982.
25. Y. R. Kwon, V. M. Hietala, and K. S. Champlin, Quasi-TEM analysis of “slow-wave” mode propagation on coplanar microstructure MIS transmission lines, *IEEE Trans. Microw. Theory Tech.,* **MTT-35**: 545–551, 1987.
26. H. Y. Lee and T. Itoh, Phenomenological loss equivalence method for planar quasi-TEM transmission lines with a thin normal conductor or superconductor, *IEEE Trans. Microw. Theory Tech.,* **MTT-37**: 1904–1909, 1989.
27. T. Kitazawa and R. Mittra, An investigation of striplines and finlines with periodic stubs, *IEEE Trans. Microw. Theory Tech.,* **MTT-32**: 684–688, 1984.
28. F. J. Glandorf and I. Wolff, A spectra-domain analysis of periodically nonuniform microstrip lines, *IEEE Trans. Microw. Theory Tech.,* **MTT-35**: 336–343, 1987.
29. K. Wu, V. Dzougaiev, and P. Saguet, Complete theoretical and experimental analysis on properties of planar periodic waveguides, *IEE Proc.,* **135**: 27–33, 1988.
30. K. Wu et al., The influence of finite conductor thickness and conductivity on fundamental and higher order modes in Miniature Hybrid MIC’s (MHMIC’s) and MMIC’s, *IEEE Trans. Microw. Theory Tech.,* **MTT-41**: 421–430, 1993.
31. K. Wu, New prospective coplanar metal-insulator-semiconductor (MIS) monolithic structure, *Electron. Lett.,* **24** (5): 262–264, 1988.
32. K. Wu and R. Vahldieck, Hybrid-mode analysis of homogeneously and inhomogeneously doped low-loss slow-wave coplanar transmission lines, *IEEE Trans. Microw. Theory Tech.,* **MTT-39**: 1348–1360, 1991.
33. C.-Y. E. Tong and K. Wu, Propagation characteristics of thin film superconducting microstrip line for terahertz applications, *Electron. Lett.,* **27**: 2299–2300, 1991.
34. C. M. Krowne and E. J. Cukauskas, GaAs slow-wave phase shifter characteristics at cryogenic temperature, *IEEE Trans. Electronic Devices* **ED-34**: 124–129, 1987.
35. W. Heinrich and H. L. Hartnagel, Wave propagation on MESFET electrodes and its influence on transistor gain, *IEEE Trans. Microw. Theory Tech.,* **MTT-35**: 1–8, 1987.
36. K. S. Giboney, M. J. W. Rodwell, and J. E. Bowers, Traveling-wave photodetector theory, *IEEE Trans. Microw. Theory Tech.,* **MTT-45**: 1310–1319, 1997.
37. M. J. Lancaster et al., Miniature superconducting filters, *IEEE Trans. Microw. Theory Tech.,* **MTT-44**: 1339–1346, 1996.
38. H. Hasegawa and S. Seki, Analysis of interconnection delay on very high-speed LSI/VLSI chips using an MIS microstrip line model, *IEEE Trans. Microw. Theory Tech.,* **MTT-32**: 1721–1727, 1984.

KE WU
École Polytechnique de Montréal

SMALL BUSINESSES. See ENTREPRENEURING.